

# Anomalous Change of Bond Energies in the Cluster Ion $\text{N}_2\text{H}^+(\text{H}_2)_n$

Kenzo Hiraoka,\* Jun Katsuragawa, and Akihito Minamitsu

Faculty of Engineering, Yamanashi University, Takeda-4, Kofu 400, Japan

Edgar W. Ignacio

Department of Chemistry, College of Science and Mathematics, MSU-Iligan Institute of Technology, Iligan City 9200, Philippines

Shinichi Yamabe\*

Department of Chemistry, Nara University of Education, Takabatake-cho, Nara 630, Japan

Received: October 1, 1997; In Final Form: December 1, 1997

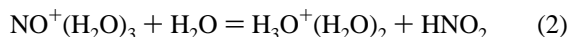
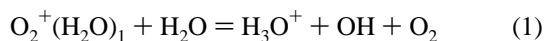
Gas-phase clustering reactions  $\text{N}_2\text{H}^+(\text{H}_2)_{n-1} + \text{H}_2 = \text{N}_2\text{H}^+(\text{H}_2)_n$  with  $n = 1-13$  were studied using a pulsed-electron beam mass spectrometer. Anomalous changes of binding energies in the cluster ion  $\text{N}_2\text{H}^+(\text{H}_2)_n$  were observed, i.e., the bond energies of  $\text{N}_2\text{H}^+(\text{H}_2)_n$  increase with  $n = 2 \rightarrow 5$ . The molecular orbital (MO) calculation revealed that the charge transfer takes place in the cluster ion  $\text{N}_2\text{H}^+(\text{H}_2)_n$  from the  $\text{H}_2$  ligands to the  $\text{N}_2\text{H}^+$  moiety, with increase of  $n$  leading to the self-tightening of the bonds in the cluster ions. The experimental bond energies of  $\text{N}_2\text{H}^+(\text{H}_2)_n$  ( $n = 2-7$ ) were reproduced by the ab initio MO calculations. The larger cluster ions  $\text{N}_2\text{H}^+(\text{H}_2)_n$  ( $n = 10-13$ ) were found to coexist with smaller ones with  $n = 6-9$  in the temperature region of 65–40 K. This suggests the presence of the structural isomers.

## 1. Introduction

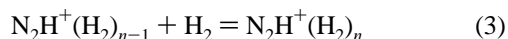
In many cases, the nature of bonding of the cluster ions changes drastically with the growth of the cluster size. For example,  $\text{H}_5^+$  in its lowest-energy conformation is not qualitatively described as  $\text{H}_3^+\cdots\text{H}_2$  but rather of  $D_{2d}$  symmetry. But the larger molecular cluster ions fit a qualitative picture  $\text{H}_3^+(\text{H}_2)_n$  with  $\text{H}_3^+$  as a nucleating center.<sup>1</sup> The electrostatic interaction between the core ion  $\text{H}_3^+$  and the  $\text{H}_2$  ligands becomes energetically more favorable than the charge dispersal in the larger clusters.

Recent calculations predicted that all five C–H bonds in the free  $\text{CH}_5^+$  are effectively equivalent and exchange dynamically rapidly, i.e.,  $\text{CH}_5^+$  is a highly fluxional molecule without a definite structure.<sup>2–4</sup> A recent infrared spectroscopic measurement for the cluster  $\text{CH}_5^+(\text{H}_2)_n$  with  $n = 0-6$  using the vibrational predissociation method revealed that the structure of the core ion  $\text{CH}_5^+$  changes from the fluxional structure to the structure with three-center–two-electron bond with the growth of the cluster size  $n = 0-6$ .<sup>5</sup>

In the high-altitude atmosphere (D-region),  $\text{O}_2^+$  and  $\text{NO}^+$  are replaced by the water cluster ions,  $\text{H}_3\text{O}^+(\text{H}_2\text{O})_n$ , through reactions 1 and 2.<sup>6</sup>



In this work, the equilibrium for the gas-phase clustering reaction (3) was measured.



Anomalous van't Hoff plots have been obtained. This anomaly

has been verified by theoretical calculations. Bond energies change irregularly as  $n$  becomes large. This unprecedented result will be explained in terms of the electronic structure of  $\text{H}^+\text{N}_2$ .

## 2. Experimental and Computation Sections

The experiments were performed with a pulsed-electron beam mass spectrometer which has been described previously.<sup>7,8</sup> The main chamber for the ion source was evacuated using a magnetic levitation turbo molecular pump (Seiko Seiki KK, STP-2000, 1950 L/s for  $\text{N}_2$ ). The ions escaping from the field-free ion source into an evacuated region were mass analyzed by a quadrupole mass spectrometer (ULVAC, MSQ-400,  $m/z = 1-550$ ). The ion counts were collected in a multichannel analyzer as a function of their arrival time after the electron pulse. The collected ions counts were transferred to the microcomputer, and the time profile of the logarithm intensities was recorded with an  $x$ – $y$  plotter. The intensity of a given ion is assumed to be proportional to the concentration (i.e., partial pressure) of that ion.

The UHP grade  $\text{H}_2$  gas (Iwatani Co. LTD, 99.99999% pure) was passed through GASCLEAN (Nikka Seikou) at atmospheric pressure in order to eliminate oxygen. The deoxygenated reagent  $\text{H}_2$  gas was passed through a molecular sieve (3 Å) trap at liquid  $\text{N}_2$  temperature at a few Torr in order to eliminate impurities and was fed into the ion source. The reagent gas contained a trace amount of  $\text{N}_2$  which produced  $\text{N}_2\text{H}^+$  by the proton-transfer reaction,  $\text{H}_3^+ + \text{N}_2 = \text{N}_2\text{H}^+ + \text{H}_2$ .

All electronic structure calculations were carried out using the GAUSSIAN 94 program system.<sup>9</sup> Geometries of  $\text{N}_2\text{H}^+(\text{H}_2)_n$  ( $n = 1-7$ ) clusters were optimized (without symmetry constraint) using the Moeller–Plesset perturbation theory truncated at second order (MP2) and using the 6-31G\*\* 6d basis

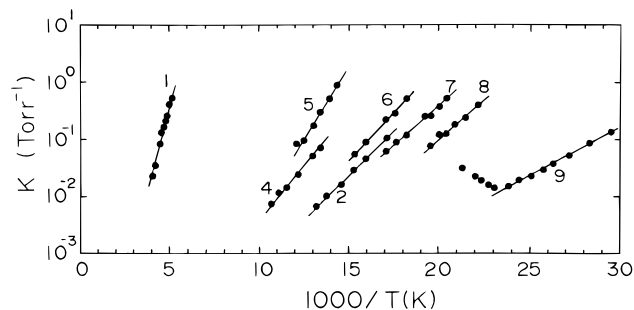


**Figure 1.** van't Hoff plots for the clustering reaction of  $\text{N}_2\text{H}^+(\text{H}_2)_{n-1} + \text{H}_2 = \text{N}_2\text{H}^+(\text{H}_2)_n$  with  $n = 1-9$ . Integer numbers attached to plots denote values of  $n$ .

**TABLE 1: Thermochemical Data  $\Delta H_{n-1,n}^\circ$  (kcal/mol) and  $\Delta S_{n-1,n}^\circ$  (cal/mol K) (Standard State, 1 atm) for Gas-Phase Clustering Reactions,  $\text{N}_2\text{H}^+(\text{H}_2)_{n-1} + \text{H}_2 = \text{N}_2\text{H}^+(\text{H}_2)_n^a$  and  $\text{H}_3^+(\text{H}_2)_{n-1} + \text{H}_2 = \text{H}_3^+(\text{H}_2)_n^b$**

$n$	$\text{N}_2\text{H}^+(\text{H}_2)_n$		$\text{H}_3^+(\text{H}_2)_n$	
	$-\Delta H_{n-1,n}^\circ$	$-\Delta S_{n-1,n}^\circ$	$-\Delta H_{n-1,n}^\circ$	$-\Delta S_{n-1,n}^\circ$
1	5.9 (6.82) <sup>c</sup>	18	6.9	17.4
	7.2 <sup>b</sup> [6.03] <sup>c</sup>	22.6 <sup>b</sup>		
2	1.4 (1.60)	15	3.31	17.4
	1.5 <sup>b</sup> [1.10]	14 <sup>b</sup>		
3	(1.61)		3.16	18.5
	[1.12]			
4	1.6 (1.78)	13	1.72	17.9
5	2.4 (1.84)	21	1.64	18.9
6	1.5 (1.67)	16	1.54	20.0
7	1.2 (1.38)	13	0.88	16.5
8	1.2	19	0.80	17.9
9	0.8	15	0.61	19.1
	isomer			
10	1.4	13		
11	1.3	13		
12	1.2	13		
13	0.9	18		

<sup>a</sup> Experimental errors for  $\Delta H_{n-1,n}^\circ$  and  $\Delta S_{n-1,n}^\circ$  are 0.2 kcal/mol and 2 cal/mol K, respectively. <sup>b</sup> References 8 and 12. <sup>c</sup> Energies in parentheses are present theoretical MP4/6-311G\*\* data. Those in square brackets are present G2\* data.

set. Vibrational frequency calculations were performed at the same level of theory. Energies at the stationary points have also been calculated at the G2\* level of theory.<sup>10</sup> The modified G2 method used in this calculation employed the MP2/6-31G\*\* 6d as a starting geometry rather than the MP2/6-31G\*, hence we call it G2\*. Using these optimized geometries, with all electrons included, single-point calculations were obtained at MP2/6-311G(d,p), MP2/6-311+G(d,p), MP2/6-311(2df,p), MP2/6-311+G(3df,2p), MP4/6-311G(d,p), MP4/6-311+G(d,p), MP4/6-311G(2df,p), and QCISDT/6-311(d,p) levels. They are components of G2\* energies. The zero-point energies (ZPEs) were scaled by 0.943,<sup>11</sup> and the final G2\* enthalpy was corrected to the temperature, 76 K. G2\* calculations were done only up to  $n = 3$ . At  $n = 4-7$ , only MP4/6-311G\*\* energy calculations were carried out. All calculations were performed on the CONVEX SPP/1200/XA computer at the Information Center of Nara University of Education.

### 3. Results and Discussion

Figure 1 shows the van't Hoff plots for the clustering reaction (3). In Table 1, thermochemical values obtained from the van't Hoff plots in Figure 1 are summarized together with our previous results for  $n = 1$  and 2.<sup>12</sup> These values<sup>12</sup> are larger than the present ones. This discrepancy is considered to be

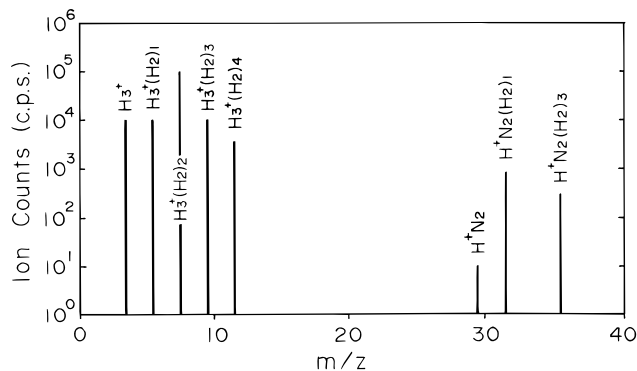


**Figure 2.** Mass spectrum obtained for 2.23 Torr  $\text{H}_2$  reagent gas containing a trace amount of a  $\text{N}_2$  impurity. Ion source temperature: 95.7 K. Electron beam: continuous mode.

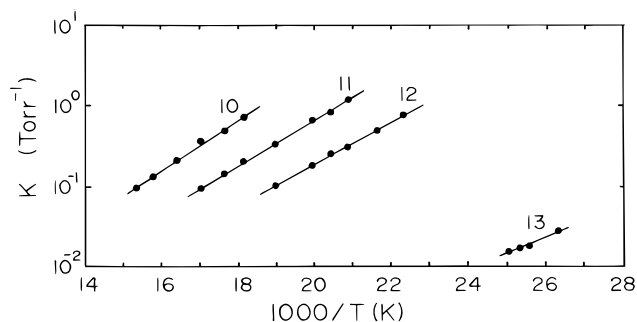
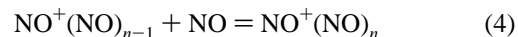


**Figure 3.** van't Hoff plots for the clustering reaction of  $\text{H}^+(\text{N}_2)_1(\text{H}_2)_{n-1} + \text{H}_2 = \text{H}^+(\text{N}_2)_1(\text{H}_2)_n$  with  $n = 10-13$ . Integer numbers attached to plots denote values of  $n$ .

due to a systematic error in the measurement of ion source temperature in our previous work.<sup>8</sup>

In Figure 1, the van't Hoff plot with  $n = 3$  is missing and those with  $n = 4$  and 5 are observed at higher temperature than that with  $n = 2$ . Such a reversal of the van't Hoff plots has never been observed except for the clustering reaction of  $\text{NO}^+$  with  $\text{NO}$ , i.e., reaction 4.<sup>13</sup>



The observed greater stability of  $\text{NO}^+(\text{NO})_n$  with even  $n$  compared to  $\text{NO}^+(\text{NO})_{n-1}$  is interpreted as the electron pairing effect of the ligand  $\text{NO}$  pair in the cluster  $\text{NO}^+(\text{NO})_n$  ( $n$ : even).

In Figure 1, the van't Hoff plot with  $n = 2$  was measured in the temperature range of 76–58 K. Below  $\sim 80$  K, the ion intensity of  $\text{N}_2\text{H}^+(\text{H}_2)_3$  was too weak for us to measure the equilibria for reaction 3 with  $n = 3$ , while strong ion signals were observed for  $\text{N}_2\text{H}^+(\text{H}_2)_n$  with  $n = 4-6$ . With the increase of ion source temperature above 80 K, the ion  $\text{N}_2\text{H}^+(\text{H}_2)_2$  disappeared and instead a strong growth of the ion  $\text{N}_2\text{H}^+(\text{H}_2)_3$  was observed. Figure 2 shows the mass spectrum obtained for 2.23 Torr  $\text{H}_2$  reagent gas at 95.7 K. Strong intensities of  $\text{H}_3^+(\text{H}_2)_n$  ions with  $n = 0-4$  together with much weaker  $\text{N}_2\text{H}^+(\text{H}_2)_n$  with  $n = 0, 1$ , and 3 were observed. It should be noted that the ion  $\text{N}_2\text{H}^+(\text{H}_2)_2$  is absent in the spectrum. This suggests that the  $\text{N}_2\text{H}^+(\text{H}_2)_3$  ion is thermochemically more stable than the smaller  $\text{N}_2\text{H}^+(\text{H}_2)_2$  ion. This is an unusual result because in general the bond energies of cluster ions decrease with the growth of the cluster size due to the less favorable electrostatic interactions. The observed anomaly is ascribed to the charge redistribution as described in the theoretical section.

In Figure 1, the van't Hoff plot with  $n = 5$  has been observed at higher temperature than that with  $n = 4$ . This reversal

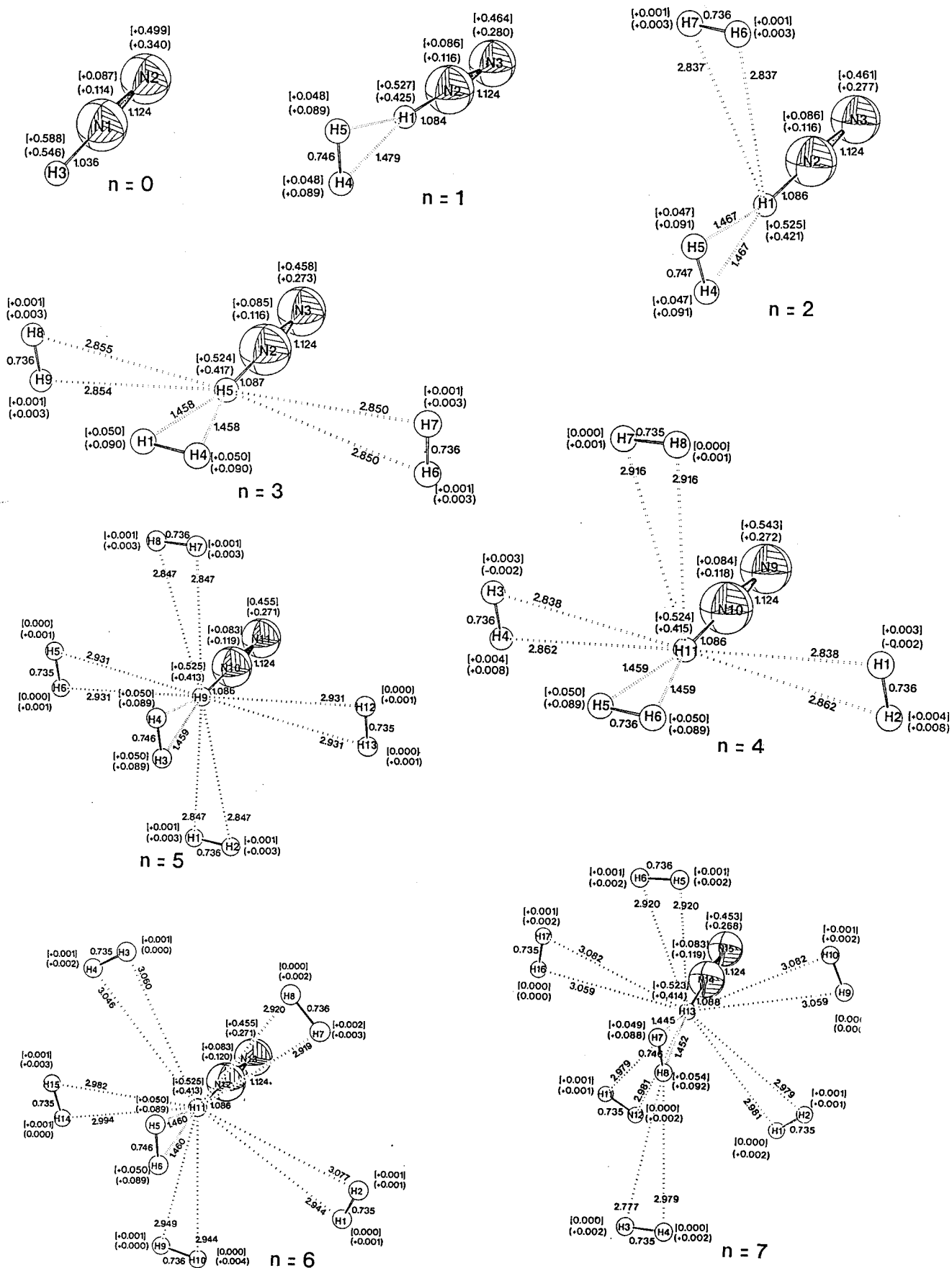
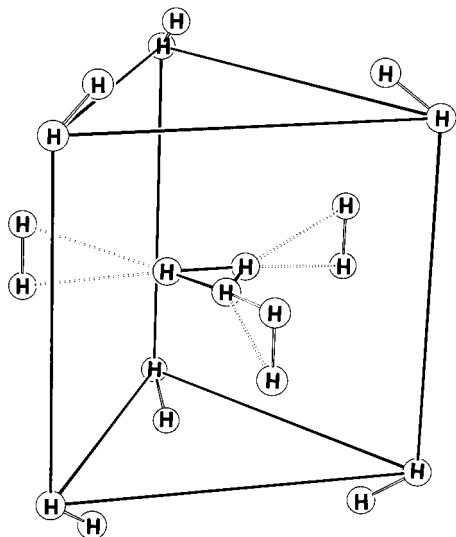


**Figure 4.** Geometries of  $N_2H^+(H_2)_n$  ( $n = 0-7$ ) optimized with MP2/6-31G\*\*6d. Distances are in angstroms. Numbers in parentheses denote Mulliken electronic charges (positive, cationic), and those in square brackets denote charges of the NBO analysis.<sup>15-17</sup>

indicates that the cluster  $N_2H^+(H_2)_4$  is less stable than the larger  $N_2H^+(H_2)_5$ . This is also due to the charge redistribution in the

cluster ions. In Figure 1, there appears a gap between  $n = 8-9$ , suggesting the shell formation with  $n = 8$ . For  $H_3^+(H_2)_n$ , the

first shell is  $H_3^+(H_2)_3$ , the second one is  $H_3^+(H_2)_6$ , and the third one is  $H_3^+(H_2)_9$ .<sup>14</sup> However, the structure of the  $N_2H^+(H_2)_8$  shell



is entirely different from that found in the  $H_3^+(H_2)_n$  cluster (see the latter section).

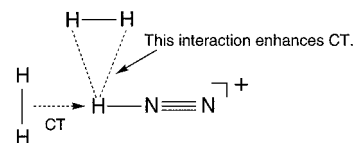
As shown in Figure 1, the measurement of the van't Hoff plots for reaction 3 ranges from 250 to 34 K for  $n = 1-9$ . In the temperature range of 64–37 K ( $1000/T = 16-27$ ), weaker signals of ions with  $m/z = 49, 51, 53,$  and  $55$  were observed. The values of these  $m/z$  correspond to those for  $N_2H^+(H_2)_n$  with  $n = 10-13$ . It is peculiar that those ions coexist with  $N_2H^+(H_2)_n$  with  $n = 6-9$  in the same temperature region (see Figure 1). At first, we thought that the appearance of those ions was due to the presence of some impurities. However, impurities other than  $N_2$  are less likely under the present experimental conditions as mentioned in the experimental section. The only possibility may be the contamination of the reagent gas with  $O_2$ . That is, those cluster ions have an  $O_2$  ligand, i.e.,  $H^+(O_2)_1(H_2)_n$  with  $n = 8-11$ . In order to examine this possibility, we intentionally added a small amount of  $O_2$  into the ultrapure  $H_2$  reagent gas through a stainless steel capillary (0.1 mm  $\phi \times 3$  m in length). We found that the introduction of  $O_2$  up  $\sim 10^{-2}$  mTorr did not lead to the increase of ions with  $m/z = 49-55$  at all. The inertness of  $O_2$  in the reagent gas is reasonable because the proton affinity of  $O_2$  is almost the same with  $H_2$  and the formation of  $O_2H^+$  as a nucleating core is unlikely. With the addition of higher pressure of  $O_2$ , strong signals of  $H^+(O_2)_2$  and their clusters with  $H_2$  ligands started to be observed, but again the intensities of ions with  $m/z = 49-55$  were not affected. From these experimental facts, we concluded that the ions with  $m/z = 49-55$  are not due to the formation of  $H^+(O_2)_1(H_2)_n$  with  $n = 8-11$  but due to the formation of isomeric  $H^+(N_2)_1(H_2)_n$  with  $n = 10-13$ .

The van't Hoff plots for reaction 3 with  $n = 10-13$  are displayed in Figure 3. The thermochemical data for these reactions are summarized in Table 1. The positive charge (cationic) in the core ion of the smaller clusters  $N_2H^+(H_2)_n$  with  $n = 6-9$  must be more dispersed than that of the isomeric clusters with  $n = 10-13$  observed in the same temperature region. This is because the ligands in the former clusters experience weaker electrostatic interactions with the core ion.

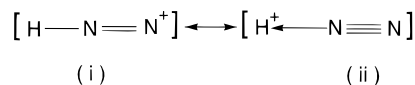
In the van't Hoff plots in Figure 3, there appears a gap between  $n = 12$  and  $13$ , i.e., the shell formation at  $n = 12$ . The broken van't Hoff plots observed with  $n = 9$  in Figure 1 may be due to the existence of the isomeric cluster ions.

#### 4. Calculation Results and Discussion

Geometries of  $HN_2^+(H_2)_n$  ( $n = 0-7$ ) are examined theoretically in Figure 4.  $HN_2^+$  ( $n = 0$ ) is a linear molecule where the cationic character is not localized on the proton. When a hydrogen molecule is attached to  $HN_2^+$ , an  $n = 1$  complex of the  $C_{2v}$  symmetry geometry has been obtained. The H–N distance is elongated as  $n = 0 \rightarrow 1$ , which reflects a charge-transfer interaction (CT),  $H_2 \rightarrow HN_2^+$ . When the second  $H_2$  molecule is attached to  $HN_2^+(H_2)_1$ , an  $n = 2$  species in Figure 4 is obtained. The  $H_2 \cdots H^+N_2(H_2)_1$  interaction is weak, but remarkable enhancement of the ( $H_2 \rightarrow HN_2^+$ ) CT is shown in the  $n = 2$  geometry. Usually, charge dispersal leads to weaken-

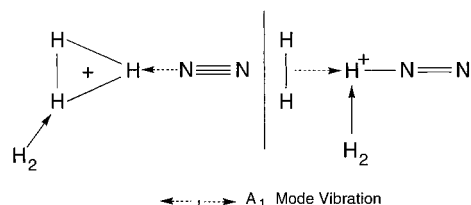


ing of interactions between a core ion and ligand neutral molecules. The remarkable bond-strength enhancement is also involved in the  $n = 3$  geometry. The enhancement effect may be explicable in terms of the following resonance structures as Mulliken and natural bond orbital (NBO)<sup>15-17</sup> electronic charges show. For small clusters, contribution of the (i) structure to the  $H_2$ -ligand capture is dominated. When clusters become large,



the cationic character is moved to the proton in the (ii) structure. The enhancement effect arises from switch of (i)  $\rightarrow$  (ii). The enhancement is completed at  $n = 5$  via  $n = 4$  (see positive charge distributions in Figure 4). The  $n = 5$  geometry is almost of  $C_{4v}$  symmetry, where the proton is coordinated by six ligands (five  $H_2$  molecules and one  $N_2$ ). Next, the  $n = 6$  geometry in Figure 4 is too crowded, which is verified by large intermolecular distances (broken lines are of almost 3 Å distances). Thus, the bond energy of the  $n = 5$  cluster is largest in the cluster ions with  $n \geq 2$ . From  $n = 7$ , the ligand  $H_2$  molecule is coordinated not to the proton but to the first  $H_2$  molecule. The second shell is completed when the two H atoms of the first  $H_2$  ligand are occupied by two  $H_2$  ligands (not shown in Figure 4). This explains the shell formation with  $n = 8$  in Figure 1.

While the  $n = 5$  shell structure is definitely determined,  $n \geq 6$  structures are very floppy. According to the  $A_1$  vibration, the position of  $H_2$  ligands would be interchangeable. Table 1



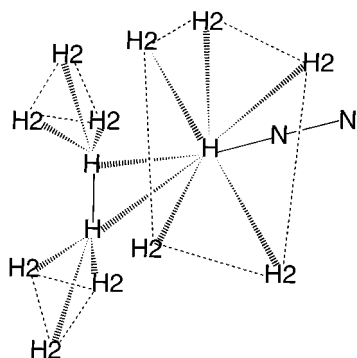
displays theoretical bond energies in parentheses and square brackets. Fair agreement between experimental and theoretical energies has been obtained. A large value  $-\Delta S_{4,5}^\circ = 21$  eu is explicable by the shell structure of  $n = 5$ .

#### 5. Concluding Remarks

The clustering reaction (3) was examined with a high-pressure mass spectrometer using an ultrapure reagent hydrogen gas

containing a very small amount of  $N_2$  impurity gas. The bond energies of  $N_2H^+(H_2)_n$  were found to increase with  $n$  with  $n = 2 \rightarrow 5$ . This anomaly is theoretically elucidated, i.e., the charge transfer from the  $H_2$  ligands to the  $H^+N_2$  moiety strengthens the interactions with the core ion  $H^+N_2$  with  $H_2$  ligands ( $n = 2 \rightarrow 5$ ). Although the most stable cluster ion is  $N_2H^+(H_2)_n$  with  $n = 5$ , the shell is formed with  $n = 6$  and 8 for the cluster ions  $(H_2)_{n-1}[H_2-H^+N_2]$ . Qualitative agreement between the experimental and theoretical bond energies is obtained.

The presence of the structural isomers of  $H^+(N_2)_1(H_2)_n$  has been suggested in the low-temperature region. There seems to be some energy barrier for the isomerization of these cluster ions. The shell completion with  $n = 12$  is predicted for the isomeric cluster ions. The enhancement effect would lead to the following shell structure.



**Acknowledgment.** We thank the Information Processing Center for Nara University of Education for the generous

allocation of CPU time on the CONVEX SPP/120/XA computer. E.W.I. thanks the DOST-ESEP for the fellowship support.

## References and Notes

- (1) Yamaguchi, Y.; Gaw, J. F.; Schaeffer, H. F., III. *J. Chem. Phys.* **1983**, *78*, 4074.
- (2) Schleyer, P. v. R.; Kim, S.-J. *J. Chem. Phys.* **1993**, *99*, 3716.
- (3) Scuseria, G. A. *Nature* **1993**, *366*, 512.
- (4) Marx, D.; Parrinello, M. *Nature* **1995**, *375*, 216.
- (5) Boo, D. W.; Lee, Y. T. *J. Chem. Phys.* **1995**, *103*, 216.
- (6) Ferguson, E. E.; Fehsenfeld, F. C.; Albritton, D. L. In *Gas Phase Ion Chemistry*; Bowers, M. T., Ed.; Academic Press, New York, 1979; 57.
- (7) Kebarle, P. In *Techniques for the Study of Ion-Molecule Reactions*; Farrar, J. M., Saunders, W. H., Eds.; Wiley: New York, 1988.
- (8) Hiraoka, K. *J. Chem. Phys.* **1987**, *87*, 4048.
- (9) Frisch, M. J.; Trucks, G. W.; Schlegel, H. B.; Gill, P. M. W.; Johnson, B. G.; Robb, M. A.; Cheeseman, J. R.; Keith, T.; Petersson, G. A.; Montgomery, J. A.; Raghavachari, K.; Al-Laham, M. A.; Ortiz, V. G.; Foresman, J. B.; Cioslowski, J.; Stefanov, B. B.; Nanayakkara, A.; Challacombe, M.; Peng, C. Y.; Ayala, P. Y.; Chen, W.; Wong, M. W.; Andres, J. L.; Replogle, E. S.; Gomperts, R.; Martin, R. L.; Fox, D. J.; Binkley, J. S.; Defrees, D. J.; Baker, J.; Stewart, J. P.; Head-Gordon, M.; Gonzalez, C.; Pople, J. A. *Gaussian 94, Revision C.4*; Gaussian, Inc.: Pittsburgh, PA, 1995.
- (10) Curtiss, L. A.; Raghavachari, K.; Trucks, G. W.; Pople, J. A. *J. Chem. Phys.*, **1991**, *94*, 7221. Curtiss, L. A.; Raghavachari, K.; Pople, J. A. *J. Chem. Phys.* **1993**, *98*, 1293.
- (11) Scott, A. P.; Radom, L. *J. Phys. Chem.* **1996**, *100*, 16502.
- (12) Hiraoka, K. *Bull. Chem. Soc. Jpn.* **1979**, *52*, 1578.
- (13) Hiraoka, K.; Minamitsu, A.; Nasu, M. *J. Chem. Phys.* **1996**, *105*, 9068.
- (14) Ignacio, E. W.; Yamabe, S. *Chem. Phys. Lett.*, submitted.
- (15) Carpenter, J. E.; Weinhold, F. *J. Mol. Struct. (THEOCHEM)* **1988**, *169*, 41.
- (16) Reed, A. E.; Curtiss, L. A.; Weinhold, F. *Chem. Rev.* **1988**, *88*, 899.
- (17) *N.B.O. Program, Version 3.1*; Glendening, E. D.; Reed, A. E.; Carpenter, J. E.; Weinhold, F.